

## Stacked Schiff Base Complexes.

### The Structural Characterization of $N,N'$ -Ethylenebis(1,1,1-trifluoro-2,4-pentanedioneiminato)copper(II) and $N,N'$ -Ethylenebis(1,1,1-trifluoro-2,4-hexanedioneiminato)nickel(II), $Cu[en(tfpd)_2]$ and $Ni[en(tfhd)_2]$

HARRY C. ALLEN, Jr.<sup>1a</sup>, GREGORY L. HILLHOUSE<sup>1b</sup>, and DEREK J. HODGSON\*

Department of Chemistry, University of North Carolina, Chapel Hill, N.C. 27514, U.S.A.

Received February 20, 1979

The crystal and molecular structures of the Schiff base complexes  $N,N'$ -ethylenebis(1,1,1-trifluoro-2,4-pentanedione)copper(II),  $Cu[en(tfpd)_2]$ ,  $CuC_{12}H_{12}N_2O_2F_6$ , and  $N,N'$ -ethylenebis(1,1,1-trifluoro-2,4-hexanedioneiminato)-nickel(II)  $Ni[en(tfhd)_2]$ ,  $NiC_{14}H_{16}N_2O_2F_6$ , have been determined from three-dimensional counter X-ray data. The copper complex crystallizes in the monoclinic space group  $P2_1/c$  in a cell of dimensions  $a = 10.665(5)$ ,  $b = 16.131(9)$ ,  $c = 9.050(4)$  Å,  $\beta = 106.43(5)^\circ$ . Least-squares refinement of the structure has led to a final R factor (on F) of 0.043 using 2351 independent intensities. The nickel complex also crystallizes in space group  $P2_1/c$  with  $a = 11.434(7)$ ,  $b = 17.798(b)$ ,  $c = 8.741(7)$  Å and  $\beta = 110.60(5)^\circ$ . Least-squares refinement of the structure, based on 1054 independent observations, has led to an R-factor (on F) of 0.073. The coordination geometry around the metal centers in both complexes is distorted square planar, the angle between the two  $N-M-O$  planes being  $13.2^\circ$  in the copper complex and  $8.5^\circ$  in the nickel complex; these results are in contrast with those reported earlier for the nickel analog of the present copper complex,  $Ni[en(tfpd)_2]$ , in which the geometry was undistorted square planar. The average  $Cu-N$  and  $Cu-O$  bond lengths are 1.939(8) and 1.909(4) Å, respectively, while the corresponding values for the  $Ni-N$  and  $Ni-O$  bonds in  $Ni[en(tfhd)_2]$  are 1.843(9) and 1.857(8) Å, respectively. Both complexes form stacks in the crystals, leading to  $Cu-Cu$  and  $Ni-Ni$  separations of 4.625(2) and 4.395(3) Å, respectively, with associated  $Cu-Cu-Cu$  and  $Ni-Ni-Ni$  angles of  $156.14(2)$  and  $167.74(8)^\circ$ , respectively. The reported EPR spectra of pure and doped complexes of this type are discussed in the light of their structures.

## Introduction

Transition metal complexes with tetradentate Schiff-base ligands have been of interest since their original synthesis. It was early recognized that the Co(II) complexes are synthetic oxygen carriers [2], and more recently they have been found to have interesting structural [3] and magnetic properties [4–7].

In particular, it has been shown through line-width anisotropy and line-shape measurements of EPR spectra that several of these complexes exhibit pseudo-one-dimensional antiferromagnetic behavior [6–8].

Of particular interest are the Cu(II) and Ni(II) complexes with  $N,N'$ -ethylenebis(1,1,1-trifluoro-pentanedioneimine)[ $en(tfpd)_2$ ] and  $N,N'$ -ethylenebis(1,1,1-trifluoro-2,4-hexanedioneimine)[ $en(tfhd)_2$ ]. Cu(II)-doped crystals of the Ni(II) complexes have been studied by EPR to yield magnetic and bonding parameters [3, 4]. The structural characterization [3] of  $Ni[en(tfpd)_2]$  revealed that the complex crystallizes such that the Ni(II) form an infinite chain. Although one-dimensional magnetic behavior has not yet been observed in this complex, this result led to the investigation of single crystals of  $Cu[en(tfpd)_2]$  that did reveal one-dimensional magnetic behavior [7]. The quantitative analysis of the magnetic behavior became possible through preliminary structural information derived from this study.

Studies on single crystals of  $Cu[en(tfhd)_2]$  showed that this complex also exhibited one-dimensional magnetic behavior [9]. Since the crystal structure of this complex was not known, the quantitative analysis of the magnetic behavior could not be carried out.

In this paper we report the structure of  $Cu[en(tfpd)_2]$  and  $Ni[en(tfhd)_2]$ . The structure of the  $Cu[en(tfhd)_2]$  was not completely determined due to crystal deterioration in the diffractometer beam.

\* Author to whom correspondence should be addressed.

However, precession and Weissenberg photography indicate that the Cu(II) and Ni(II) chelates of  $\text{en}(\text{tfhd})_2$  are isomorphous.

## Experimental

### $\text{Cu}[\text{en}(\text{tfpd})_2]$

Single crystals suitable for X-ray analysis were prepared as previously described [4]. From examination of the crystals by precession and Weissenberg photography the crystals were assigned to the monoclinic system. Systematic absences were observed for  $0k0$  with  $k$  odd and  $h0l$  with  $l$  odd which uniquely determines the space group as  $\text{P}2_1/\text{c}(\text{C}_{2h}^5)$ . The unit cell constants, obtained by least squares methods are  $a = 10.665(5)$ ,  $b = 16.131(9)$ ,  $c = 9.050(4)$  Å,  $\beta = 106.43(5)^\circ$ . The observations were made at  $20^\circ\text{C}$  with the wavelength of  $\lambda(\text{MoK}\alpha) = 0.70926$  Å. The density of  $1.68 \text{ g cm}^{-3}$  calculated for four molecules in a unit cell is in good agreement with the value  $1.66(2) \text{ g cm}^{-3}$  observed by flotation in aqueous  $\text{ZnBr}_2$ . Thus with four formula units per unit cell, no crystallographic symmetry need be imposed on the molecules.

Diffraction data were collected from a parallelepiped crystal with faces  $(1\bar{1}0)$ ,  $(\bar{1}10)$ ,  $(\bar{1}\bar{1}0)$ ,  $(110)$ ,  $(001)$  and  $(00\bar{1})$ ; the separations between opposite faces were as follows;  $(1\bar{1}0)$  and  $(\bar{1}10)$ , 0.02 cm;  $(110)$  and  $(\bar{1}\bar{1}0)$ , 0.02 cm;  $(001)$  and  $(00\bar{1})$ , 0.104 cm. The crystal was mounted approximately normal to the  $(001)$  planes, and data were collected on a Picker four-circle automatic diffractometer using  $\text{MoK}\alpha$  radiation and a graphite monochromator as previously described [3]. To allow for the presence of both  $\text{K}\alpha_1$  and  $\text{K}\alpha_2$  radiations, peaks were scanned from  $0.7^\circ$  in  $2\theta$  below the calculated  $\text{K}\alpha_1$  peak position to  $0.7^\circ$  in  $2\theta$  above the calculated  $\text{K}\alpha_2$  peak position at a scan rate of  $1.0^\circ (2\theta) \text{ min}^{-1}$ . Stationary-crystal stationary-counter backgrounds were counted for 10 s on each side of the peaks. A unique data set of 3382 reflections having  $2\theta(\text{Mo}) \leq 53^\circ$  was gathered.

The data were processed as described by Ibers and coworkers [10]. After correction for background, the data were assigned standard deviations according to the formula [10] and the value of  $p$  was assigned as

$$\sigma(I) = [C + 0.25(\text{ts}/\text{tb})^2(\text{B}_H + \text{B}_L) + (pI)^2]^{1/2}$$

0.04. The data were corrected for Lorentz-polarization effects. Of the 3382 intensities collected, only 2351 were independent data having  $I > 3\sigma(I)$ ; only these data were used in the refinement of the structure. An absorption correction was applied; the linear absorption coefficient for this compound and  $\text{MoK}\alpha$

radiation is  $15.98 \text{ cm}^{-1}$ . The transmission coefficients for the data crystal ranged between 0.644 and 0.794.

### $\text{Ni}[\text{en}(\text{tfhd})_2]$

Suitable crystals were prepared as previously described [4]. Examination by precession and Weissenberg photography revealed the crystals to belong to the monoclinic systems. Systematic absences were the same as for  $\text{Cu}[\text{en}(\text{tfpd})_2]$ , uniquely determining the space group as  $\text{P}2_1/\text{c}$ . The cell constants, determined by least squares, are  $a = 11.434(7)$ ,  $b = 17.798(6)$ ,  $c = 8.741(7)$  Å,  $\beta = 110.60(5)^\circ$ ; the observations were made at  $20^\circ\text{C}$  with  $\text{CuK}\alpha$  radiation ( $\lambda = 1.5405$  Å). The density of  $1.63 \text{ g cm}^{-3}$  calculated for four molecules per unit cell is in good agreement with the value of  $1.64(2) \text{ g cm}^{-3}$  measured by flotation in aqueous  $\text{Cd}(\text{NO}_3)_2$ .

Intensity data were collected on a parallelepiped crystal bounded by the same faces as in the  $\text{Cu}[\text{en}(\text{tfpd})_2]$  case. The separations between opposite faces were:  $(110)$  and  $(\bar{1}\bar{1}0)$ , 0.013 cm;  $(\bar{1}10)$  and  $(1\bar{1}0)$ , 0.045 cm;  $(001)$  and  $(00\bar{1})$ , 0.095 cm. The crystal was mounted approximately normal to the  $(001)$  planes. Data were collected as above using  $\text{CuK}\alpha$  radiation. A unique data set of 1658 reflections having  $2\theta(\text{Cu}) < 100^\circ$  was gathered, of which 1054 had intensities greater than three times their estimated standard deviations; only these data were used in the subsequent refinement.

The data were processed in the above manner. An absorption correction was applied, the linear absorption coefficient for this compound and  $\text{CuK}\alpha$  radiation being  $23.4 \text{ cm}^{-1}$ . The transmission coefficients for the data crystal ranged between 0.37 and 0.80.

### $\text{Cu}[\text{en}(\text{tfhd})_2]$

This chelate was prepared as previously described [4] and suitable single crystals were grown by the slow evaporation of an acetone solution. The crystals were examined by precession and Weissenberg photography. It was found that the films for this chelate were essentially superimposable over those of  $\text{Ni}[\text{en}(\text{tfhd})_2]$ . The systematic absences made it possible to determine the space group as  $\text{P}2_1/\text{c}$ . The unit cell constants are determined to be  $a = 11.46(9)$ ,  $b = 17.79(13)$ ,  $c = 8.77(6)$  Å, and  $\beta = 111.3(3)^\circ$  which agree with those obtained for the Ni complex within the experimental uncertainty. Deterioration of the crystals in the X-ray beam precluded the collection of intensity data.

## Solution and Refinement of the Structures

All least-squares refinements in these analyses were carried out on  $F$ , the function minimized being

TABLE I. Positional Parameters for Cu[en(tfpd)<sub>2</sub>].

Atom	x	y	z
Cu	-0.16091(4)	0.22036(2)	0.31901(5)
F(1)	0.2363(2)	0.1224(2)	0.2961(4)
F(2)	0.1103(3)	0.1002(2)	0.0728(3)
F(3)	0.2451(3)	0.2018(2)	0.1104(5)
F(4)	-0.2991(3)	-0.0463(2)	0.3992(5)
F(5)	-0.3794(4)	-0.0163(2)	0.1681(4)
F(6)	-0.4959(3)	-0.0125(2)	0.3203(5)
C(1)	0.1635(4)	0.1607(3)	0.1717(6)
C(2)	0.0603(3)	0.2149(2)	0.2074(4)
C(3)	0.0590(4)	0.2979(3)	0.1785(5)
C(4)	-0.0282(4)	0.3560(2)	0.2134(5)
C(5)	-0.0105(6)	0.4454(3)	0.1761(9)
C(6)	-0.3793(4)	0.0053(3)	0.3085(6)
C(7)	-0.3391(3)	0.0952(2)	0.3415(4)
C(8)	-0.4191(4)	0.1470(3)	0.3906(5)
C(9)	-0.3970(4)	0.2333(3)	0.4201(5)
C(10)	-0.4943(6)	0.2793(6)	0.4802(8)
C(11)	-0.2099(5)	0.3926(3)	0.3067(6)
C(12)	-0.2711(5)	0.3592(3)	0.4241(6)
N(1)	-0.1185(3)	0.3329(2)	0.2777(4)
N(2)	-0.2964(3)	0.2701(2)	0.3958(4)
O(1)	-0.0171(2)	0.1724(1)	0.2639(3)
O(2)	-0.2289(2)	0.1106(1)	0.3164(3)
H(3)	0.119(4)	0.319(2)	0.145(5)
H(5A)	0.043(8)	0.457(5)	0.107(11)
H(5B)	0.024(6)	0.468(4)	0.297(8)
H(5C)	-0.087(6)	0.476(4)	0.142(7)
H(8)	-0.499(4)	0.121(2)	0.411(5)
H(11A)	-0.173(4)	0.445(3)	0.338(5)
H(11B)	-0.292(5)	0.407(3)	0.195(6)
H(12A)	-0.198(5)	0.365(3)	0.528(7)
H(12B)	-0.353(4)	0.391(2)	0.420(5)
H(10A)	-0.542(6)	0.313(3)	0.412(7)
H(10B)	-0.547(7)	0.257(5)	0.453(9)
H(10C)	-0.448(5)	0.317(3)	0.604(7)

TABLE II. Positional Parameters for Ni[en(tfhd)<sub>2</sub>].

Atom	x	y	z
Ni	0.1802(2)	0.2632(1)	0.1867(2)
N(1)	0.3031(9)	0.2114(5)	0.1385(10)
N(2)	0.1233(10)	0.1713(5)	0.2260(11)
O(1)	0.2477(8)	0.3576(4)	0.1784(10)
O(2)	0.0524(8)	0.3171(4)	0.2192(9)
C(1)	0.3956(14)	0.4494(7)	0.1926(21)
C(2)	0.3544(13)	0.3690(6)	0.1695(14)
C(3)	0.4331(11)	0.3147(7)	0.1430(14)
C(4)	0.4056(11)	0.2372(6)	0.1244(13)
C(5)	0.4978(14)	0.1904(7)	0.0882(18)
C(6)	0.5958(14)	0.1651(7)	0.2567(21)
C(7)	-0.0974(14)	0.0378(8)	0.2069(18)
C(8)	0.0047(13)	0.0796(7)	0.3392(16)
C(9)	0.0278(13)	0.1593(6)	0.2803(16)
C(10)	-0.0510(12)	0.2149(6)	0.2911(15)
C(11)	-0.0370(12)	0.2888(7)	0.2574(14)
C(12)	-0.1300(14)	0.3470(7)	0.2559(20)
C(13)	0.2690(11)	0.1322(6)	0.1039(16)
C(14)	0.2030(12)	0.1097(6)	0.2120(16)
F(1)	0.5029(9)	0.4627(4)	0.1787(14)
F(2)	0.4002(8)	0.4751(4)	0.3356(10)
F(3)	0.3155(8)	0.4934(4)	0.0851(9)
F(4)	-0.2085(10)	0.3232(5)	0.3254(16)
F(5)	-0.1904(10)	0.3751(7)	0.1193(13)
F(6)	-0.0776(8)	0.4053(4)	0.3466(12)
H(3)	0.511	0.333	0.141
H(10)	-0.121	0.202	0.325
H(5A)	0.539	0.218	0.030
H(5B)	0.459	0.147	0.024
H(8A)	0.082	0.050	0.371
H(8B)	-0.015	0.084	0.439
H(13A)	0.345	0.101	0.129
H(13B)	0.219	0.123	-0.005
H(14A)	0.262	0.098	0.323
H(14B)	0.153	0.065	0.175

$\sum w(|F_o| - |F_c|)^2$  with the weights  $w$  assigned as  $4F_o^2/\sigma^2(F_o^2)$ . In all calculations of  $F_c$  the atomic scattering factors for non-hydrogen atoms were from International Tables [11] while those for hydrogen were from Stewart *et al.* [12]. The effects of the anomalous dispersion of the Ni and Cu atoms were included in the calculation of  $F_c$ , the values of  $\Delta f'$  and  $\Delta f''$  being taken from the tabulation of Cromer and Liberman [13].

#### Cu[en(tfpd)<sub>2</sub>]

The position of the copper atom was deduced from a three-dimensional Patterson function, and the remaining non-hydrogen atoms were located after subsequent least-squares iterations and difference Fourier summations. Isotropic refinement of these atoms gave values of the usual agreement factors  $R_1 = \sum \|F_o - F_c\|/\sum |F_o|$  and  $R_2$  (or weighted

R-factor) =  $[\sum w(|F_o| - |F_c|)^2/\sum w(F_o)^2]^{1/2}$  of 0.116 and 0.186, respectively. Anisotropic refinement reduced these values to 0.062 and 0.078, respectively. The hydrogen atoms were located in difference Fourier maps, and subsequent least-squares calculations involved anisotropic refinement of the non-hydrogen atoms and isotropic refinement of the hydrogen atoms. The final values of  $R_1$  and  $R_2$ , derived from 2351 observations and 256 variables, were 0.043 and 0.051, respectively. In the final least-squares cycle, no atomic parameter experienced a shift greater than  $0.35\sigma$ , which is taken as evidence of convergence. Examination of the values of  $|F_o|$  and  $|F_c|$  suggested that no correction for secondary extinction was necessary. A final difference Fourier map was featureless, with no peak higher than  $0.6 \text{ e}\text{\AA}^{-3}$ . The final atomic positional parameters, together with their standard deviations as estimated

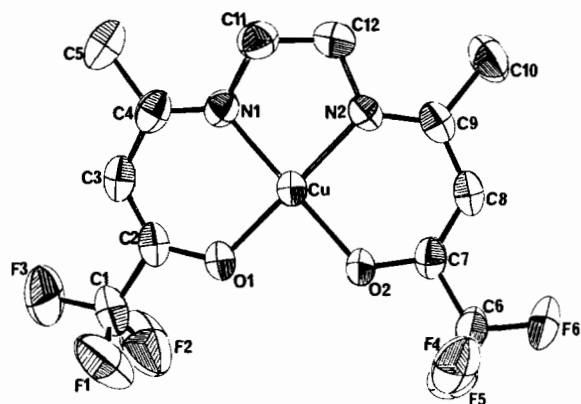


Fig. 1. View of a single molecule of  $\text{Cu}[\text{en}(\text{tfpd})_2]$  showing the atomic numbering scheme. Hydrogen atoms have been omitted. Thermal parameters are drawn at the 40% probability level.

from the inverse matrix, are listed in Table I. Observed and calculated structure amplitudes and the final thermal parameters are available [14].

#### $\text{Ni}[\text{en}(\text{tfhd})_2]$

The position of the nickel atom was deduced from a three-dimensional Patterson function. The remaining non-hydrogen atoms were located in subsequent difference Fourier maps, and after two cycles of least-squares using isotropic thermal parameters the residuals were  $R_1 = 0.148$  and  $R_2 = 0.192$ . Two additional cycles of least-squares refinement with anisotropic thermal parameters for all 25 non-hydrogen atoms gave  $R_1 = 0.092$  and  $R_2 = 0.115$ . In the following difference Fourier map it was possible to locate only one of the ring hydrogen atoms. Consequently, the hydrogen atoms whose positions could be calculated were placed in their theoretical positions based on the expected geometry at the carbon atoms (*i.e.* tetrahedral geometry at the methylene carbon atoms, trigonal geometry at the ring carbon atoms, all C–H bond lengths assigned as 0.95 Å); these hydrogen contributions were included in subsequent least-squares cycles, but the hydrogen atom coordinates were not varied. Attempts to locate the methyl hydrogen atoms were unsuccessful, so these atoms were omitted for the calculation. In the final cycle of least-squares refinement no parameter showed a shift of more than 0.006 times its estimated standard deviation which was taken as evidence that the refinement had converged. The final cycle of least squares involved full-matrix refinement of 227 variables using 1054 independent intensities. The final values of the residuals are  $R_1 = 0.073$  and  $R_2 = 0.093$ . The positional parameters for all atoms are given in Table II. Tables of observed and calculated structural amplitudes and anisotropic thermal parameters are available.

TABLE III. Internuclear Distances (Å) in  $\text{M}[\text{en}(\text{tfpd})_2]$ ,  $\text{M} = \text{Ni}, \text{Cu}$ .

Bond	M = Cu	M = Ni <sup>a</sup>
M–O(1)	1.906(3)	1.839(4)
M–O(2)	1.911(3)	1.848(4)
M–N(1)	1.933(3)	1.864(5)
M–N(2)	1.944(3)	1.856(4)
C(1)–F(1)	1.325(5)	1.311(7)
C(1)–F(2)	1.337(5)	1.319(6)
C(1)–F(3)	1.334(5)	1.319(8)
C(6)–F(4)	1.305(5)	1.306(7)
C(6)–F(5)	1.317(6)	1.315(8)
C(6)–F(6)	1.310(6)	1.313(8)
C(1)–C(2)	1.512(6)	1.539(8)
C(6)–C(7)	1.518(6)	1.515(8)
O(1)–C(2)	1.285(4)	1.283(6)
O(2)–C(7)	1.282(6)	1.274(7)
C(2)–C(3)	1.363(5)	1.330(7)
C(7)–C(8)	1.357(6)	1.356(7)
C(3)–C(4)	1.418(6)	1.429(8)
C(8)–C(9)	1.424(6)	1.431(8)
C(4)–C(5)	1.505(6)	1.526(8)
C(9)–C(10)	1.497(7)	1.524(8)
N(1)–C(4)	1.313(5)	1.303(7)
N(2)–C(9)	1.298(5)	1.299(7)
N(1)–C(11)	1.446(5)	1.435(7)
N(2)–C(12)	1.472(5)	1.465(7)
C(11)–C(12)	1.496(6)	1.412(9)
M–M	4.625(2)	4.024(3)

<sup>a</sup>Data for  $\text{Ni}[\text{en}(\text{tfpd})_2]$  are from reference 3.

#### Description of the Structures

##### $\text{Cu}[\text{en}(\text{tfpd})_2]$

The structure consists of a stacked arrangement of the  $\text{Cu}[\text{en}(\text{tfpd})_2]$  molecules resulting in the formation of infinite chains of Cu(II). The interionic separation in the chain is 4.625(2) Å. The chain of copper ions is kinked, with a Cu–Cu–Cu angle of 156.14(2)°. The trifluoromethyl groups are symmetrically disposed and the condensation occurred in the 4-position, as was found for the Ni(II) chelate [3]. The geometry and numbering scheme are shown in Fig. 1; bond lengths and bond angles are compared with those in the nickel analog in Tables III and IV, respectively.

The average Cu–O and Cu–N bond lengths, 1.909 and 1.939 Å, are close to the values found in other Cu(II) Schiff-base chelates in which the metal ions form linear chains [15–17], and show no large deviations between the two Cu–O and Cu–N bonds as seem to be present when the chelates crystallize as dimers [18, 19]. The bond lengths in the macrocycle are about the same as those found in the non-fluorinated analog [19, 20] and are comparable to those found in similar complexes where the ligand is  $\text{en}(\text{pd})_2$  [19–21]. The C–C bond adjacent to the

TABLE IV. Intramolecular Angles ( $^{\circ}$ ) in  $M[\text{en}(\text{tfpd})_2]$ ,  $M = \text{Cu}, \text{Ni}$ .

Bonds	$M = \text{Cu}$	$M = \text{Ni}^a$
O(1)–M–O(2)	87.2(1)	83.4(2)
O(1)–M–N(1)	94.6(1)	95.0(2)
O(1)–M–N(2)	174.4(1)	177.9(5)
O(2)–M–N(1)	167.6(1)	177.2(2)
O(2)–M–N(2)	93.9(1)	94.5(2)
N(1)–M–N(2)	85.4(1)	87.0(2)
M–O(1)–C(2)	122.9(2)	124.0(3)
M–O(2)–C(7)	122.7(2)	124.4(4)
O(1)–C(2)–C(3)	128.9(4)	128.3(5)
O(2)–C(7)–C(8)	129.1(4)	128.5(5)
O(1)–C(2)–C(1)	111.4(3)	111.4(5)
O(2)–C(7)–C(6)	111.9(3)	112.8(5)
C(1)–C(2)–C(3)	119.7(4)	120.3(5)
C(6)–C(7)–C(8)	119.0(3)	118.7(5)
C(2)–C(3)–C(4)	125.3(4)	123.6(5)
C(7)–C(8)–C(9)	125.3(3)	122.5(5)
C(3)–C(4)–N(1)	121.4(3)	121.2(5)
C(8)–C(9)–N(2)	121.1(3)	121.6(5)
C(3)–C(4)–C(5)	116.8(4)	117.0(5)
C(8)–C(9)–C(10)	117.2(5)	116.8(5)
N(1)–C(4)–C(5)	121.8(4)	121.8(6)
N(2)–C(9)–C(10)	121.7(3)	121.6(5)
M–N(1)–C(4)	126.4(3)	126.9(4)
M–N(2)–C(9)	127.2(3)	127.7(4)
M–N(1)–C(11)	112.5(3)	113.0(4)
M–N(2)–C(12)	110.3(3)	112.6(4)
C(4)–N(1)–C(11)	120.6(3)	120.0(5) <sup>b</sup>
C(9)–N(2)–C(12)	122.4(3)	119.6(5) <sup>b</sup>
N(1)–C(11)–C(12)	110.0(3)	114.0(5) <sup>b</sup>
N(2)–C(12)–C(11)	108.8(3)	112.6(5) <sup>b</sup>
F(1)–C(1)–F(2)	105.3(4)	106.1(5)
F(1)–C(1)–F(3)	106.9(4)	107.0(6)
F(2)–C(1)–F(3)	106.8(4)	107.0(6)
F(4)–C(6)–F(5)	105.1(5)	107.2(6)
F(4)–C(6)–F(6)	106.1(4)	106.6(6)
F(5)–C(6)–F(6)	106.3(4)	106.0(6)

<sup>a</sup>Data for  $\text{Ni}[\text{en}(\text{tfpd})_2]$  from reference 3. <sup>b</sup>Calculated from data in reference 3.

C–O bond is shorter than the C–C bond adjacent to the C–N bond, which is characteristic of this type of chelate since the former is formally a double bond. The C–C bond in the bridging ethylene moiety is somewhat longer than that reported [3] for  $\text{Ni}[\text{en}(\text{tfpd})_2]$ . All chemically equivalent bond lengths in the structure are in excellent agreement with the exception of N(1)–C(11) and N(2)–C(12) which differ by somewhat more than  $5\sigma$ . This latter difference has been found previously in similar complexes [3, 19]. The six independent C–F distances in the  $\text{CF}_3$  groups lie in the range 1.305(5)–1.337(5) Å, which is in the range found in other trifluoromethyl-containing complexes [3, 22, 23].

The coordination sphere is not planar but tetrahedrally distorted as evidenced by the  $13.2^{\circ}$  angle

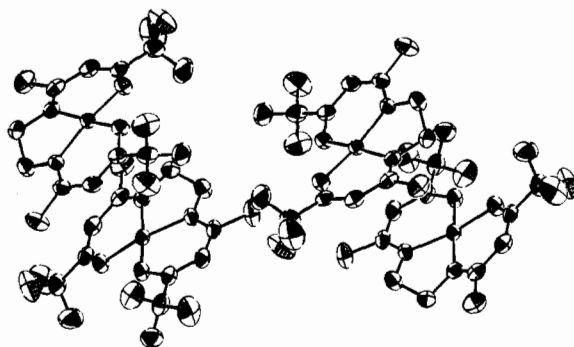


Fig. 2. View of the molecular packing in the crystals of  $\text{Cu}[\text{en}(\text{tfpd})_2]$ . The view is normal to the  $a^*$ -axis.

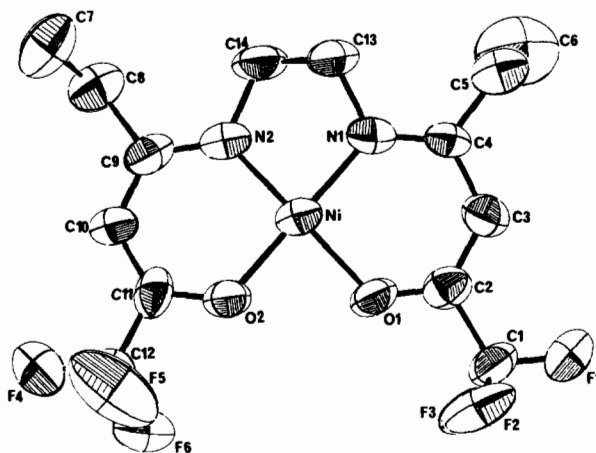


Fig. 3. View of a single molecule of  $\text{Ni}[\text{en}(\text{tfhd})_2]$  showing the atomic numbering scheme. Hydrogen atoms have been omitted. Thermal parameters are drawn at the 40% probability level.

between the planes formed by N(1)–Cu–O(1) and N(2)–Cu–O(2). The N(1), O(2) atoms lie 0.15 Å above the best plane through N(1), N(2), O(1), O(2) while the N(2), O(1) atoms lie 0.15 Å below it. Unlike the situation in  $\text{Ni}[\text{en}(\text{tfpd})_2]$  [3] and  $\text{Cu}[\text{en}(\text{pd})_2]$  [18, 20], the bridging carbon atoms are located trans with respect to the best plane through the coordinating atoms with C(11) located 0.26 Å above the plane and C(12) located 0.41 Å below the plane.

The two six-membered chelate rings are essentially planar, but in addition to the tetrahedral distortion about the copper atom the macrocycle as a whole is folded about an axis that bisects the N(1)–Cu–N(2) angle. The sum of these two distortions results in an angle of  $20.7^{\circ}$  between the normals to the two chelate rings.

The crystal packing of the chelates is shown in Fig. 2. Although not required crystallographically, the molecular planes are nearly parallel, thus allowing the formation of the infinite chains that give

TABLE V. Internuclear Distances (Å) in Ni[en(tfhd)<sub>2</sub>].

Bond	Distance	Bond	Distance
Ni-O(1)	1.861(7)	Ni-O(2)	1.852(8)
Ni-N(1)	1.849(9)	Ni-N(2)	1.837(9)
N(1)-C(4)	1.30(1)	N(2)-C(9)	1.35(2)
N(1)-C(13)	1.47(1)	N(2)-C(14)	1.46(1)
O(1)-C(2)	1.27(1)	O(2)-C(11)	1.29(1)
C(1)-C(2)	1.50(2)	C(11)-C(12)	1.48(2)
C(2)-C(3)	1.40(2)	C(10)-C(11)	1.37(2)
C(3)-C(4)	1.41(2)	C(9)-C(10)	1.36(2)
C(4)-C(5)	1.46(2)	C(8)-C(9)	1.56(2)
C(5)-C(6)	1.57(2)	C(7)-C(8)	1.52(2)
C(1)-F(1)	1.30(1)	C(12)-F(4)	1.32(2)
C(1)-F(2)	1.31(2)	C(12)-F(5)	1.25(2)
C(1)-F(3)	1.31(2)	C(12)-F(6)	1.31(1)
Ni-Ni'	4.395(3)	C(13)-C(14)	1.46(2)

rise to the observed one-dimensional magnetic behavior.

#### Ni[en(tfhd)<sub>2</sub>]

The geometry and numbering scheme are shown in Fig. 3; bond lengths and bond angles are summarized in Tables V and VI, respectively. The structure is very similar to that observed for Cu[en(tfpd)<sub>2</sub>]. The bond distances and angles are similar to those found in similar chelates. The coordinating atoms, again, do not form a good plane, for N(1) and O(2) are about 0.09 Å above the best coordina-

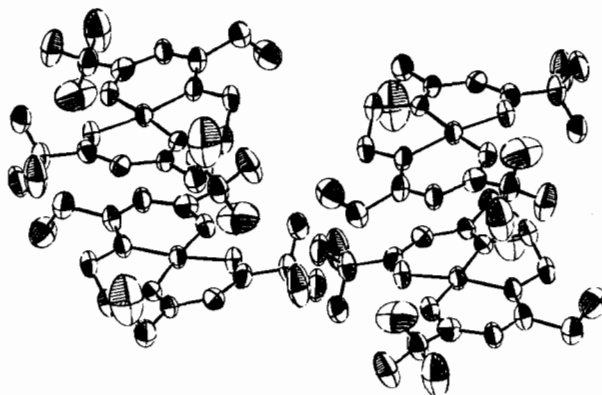


Fig. 4. View of the molecular packing in the crystals of Ni[en(tfhd)<sub>2</sub>]. The view is normal to the *a*\*-axis.

tion plane and N(2) and O(2) are about 0.10 Å below the plane. The bridging carbon atoms are again disposed trans to the best coordination plane with C(13) 0.44 Å above the plane and C(14) 0.18 Å below the plane. The angle between the two N-Ni-O planes is 8.5°, a smaller distortion than found in Cu[en(tfpd)<sub>2</sub>]. The two chelate rings are essentially planar within the accuracy of the determination. Once again there is a folding of the molecule about the bisector of the N-Ni-N angle. The combination of the two distortions results in an angle of 16.4° between the normals of the two planes.

TABLE VI. Intramolecular Angles (°) in Ni[en(tfhd)<sub>2</sub>].

Bonds	Angle	Bonds	Angle
O(1)-Ni-O(2)	84.2(4)	Ni-N(1)-C(4)	128.8(8)
O(1)-Ni-N(1)	94.7(4)	Ni-N(1)-C(13)	111.0(8)
O(1)-Ni-N(2)	172.0(4)	C(4)-N(1)-C(13)	120.1(9)
O(2)-Ni-N(1)	173.8(4)	Ni-N(2)-C(9)	126.1(8)
O(2)-Ni-N(2)	94.7(4)	Ni-N(2)-C(14)	112.4(8)
N(1)-Ni-N(2)	86.9(4)	C(9)-N(2)-C(14)	121(1)
Ni-O(1)-C(2)	124.7(7)	C(4)-C(5)-C(6)	107(1)
Ni-O(2)-C(11)	125.4(8)	C(7)-C(8)-C(9)	112(1)
O(1)-C(2)-C(3)	126(1)	N(1)-C(13)-C(14)	107(1)
O(1)-C(2)-C(1)	114(1)	N(2)-C(14)-C(13)	109(1)
C(1)-C(2)-C(3)	120(1)	C(2)-C(1)-F(1)	115(1)
O(2)-C(11)-C(10)	127(1)	C(2)-C(1)-F(2)	112(1)
O(2)-C(11)-C(12)	111(1)	C(2)-C(1)-F(3)	111(1)
C(10)-C(11)-C(12)	122(1)	F(1)-C(1)-F(2)	107(1)
C(2)-C(3)-C(4)	124(1)	F(1)-C(1)-F(3)	106(1)
C(9)-C(10)-C(11)	124(1)	F(2)-C(1)-F(3)	105(1)
C(3)-C(4)-N(1)	120(1)	C(11)-C(12)-F(4)	112(1)
C(3)-C(4)-C(5)	116(1)	C(11)-C(12)-F(5)	116(1)
N(1)-C(4)-C(5)	124(1)	C(11)-C(12)-F(6)	112(1)
C(10)-C(9)-N(2)	123(1)	F(4)-C(12)-F(5)	109(1)
C(8)-C(9)-C(10)	116(1)	F(4)-C(12)-F(6)	103(1)
N(2)-C(9)-C(8)	121(1)	F(5)-C(12)-F(6)	104(1)

TABLE VII. Structural and Magnetic Data of  $^{63}\text{Cu}$  doped Ni Chelates.

	Distortion Angle	$g_z$	$g_x$	$g_y$	$A_z^a$	$A_x^a$	$A_y^a$
$\text{Cu}[\text{en}(\text{tfpd})_2]$	0	2.192	2.048	2.046	200.8	31.1	28.3
$\text{Cu}[\text{en}(\text{tfhd})_2]$	8.5	2.198	2.048	2.046	196.8	31.5	21.3
$\text{Cu}[\text{pn}(\text{acet})_2]$		2.216	2.045	2.043	190.4	35.0	30.2

<sup>a</sup>In  $(\text{cm}^{-1} \times 10^4)$ .

Figure 4. shows the packing of the chelates. As in the previous case, the molecules stack in such a manner as to form infinite chains of the Ni(II) centers with the molecular planes nearly parallel to each other. The chains of metal ions are much more nearly linear than in the  $\text{Cu}[\text{en}(\text{tfpd})_2]$  case, with a Ni–Ni angle of  $167.74(8)^\circ$ . The Ni–Ni separation of  $4.395(3)$  Å is shorter than the Cu–Cu separation in  $\text{Cu}[\text{en}(\text{tfpd})_2]$  but longer than that of  $4.024(3)$  Å reported [3] for  $\text{Ni}[\text{en}(\text{tfpd})_2]$ .

## Discussion

There has been considerable recent interest in the correlation of magnetic properties with molecular structure. Notable experimental success has been achieved in correlating the magnetic properties of bridged copper(II) dimers with the Cu–X–Cu bridging angle,  $\phi$  [24–26], and this relationship has been explained through the application of molecular orbital theory [24, 27, 28]. Structural data are now available [3, 15] for the nickel(II) and copper(II) chelates of  $\text{en}(\text{tfpd})_2$ , for  $\text{Ni}[\text{en}(\text{tfhd})_2]$ , and for  $N,N'$ -1,3-propanebis(2-hydroxyacetophenoneiminato) copper(II),  $\text{Cu}[\text{pn}(\text{acet})_2]$ . In all of these complexes except  $\text{Ni}[\text{en}(\text{tfpd})_2]$  the central metal ion experiences a tetrahedral distortion. The amount of this distortion, which may be measured by the angle between the two N–M–O planes, is listed along with the pertinent spin-Hamiltonian parameters [7, 8] for  $^{63}\text{Cu}$ -doped single crystals of the three Ni(II) chelates and the single crystal g-values for the three Cu(II) complexes in Tables VII and VIII. In the former cases, it must be assumed that the Cu(II) dopant is forced to adopt the configuration found in the crystal for the Ni(II) ions.

McGarvey [29] has shown qualitatively that if  $\langle A \rangle$  is negative [as is normally the case for copper(II)] then it is expected to decrease as  $\langle g \rangle$  increases according to the relationship

$$\langle A \rangle = -K + (\langle g \rangle - 2.0023)P$$

where K is the isotropic hyperfine term and P is proportional to  $\langle r^{-3} \rangle$ . The deviation of  $\langle g \rangle$  from the free

TABLE VIII. Structural and Magnetic Data of Cu Complexes.

	Distortion	$g_z$	$g_x$	$g_y$
$\text{Cu}[\text{en}(\text{tfpd})_2]$	13.2	2.200	2.055	2.049
$\text{Cu}[\text{en}(\text{tfhd})_2]$		2.197	2.051	2.047
$\text{Cu}[\text{pn}(\text{acet})_2]$	37	2.225	2.052	2.048

electron value is inversely related to the ligand field strength; hence, as the distortion from square planar to tetrahedral geometry increases the value of  $\langle g \rangle$  is expected to increase since the ligand field strength decreases. These two qualitative predictions are supported by the data in Tables VII and VIII, although before any quantitative correlation can be attempted it will be necessary for more data on these and related complexes to be obtained.

## Acknowledgments

G. L. H. was supported by the William R. Kenan, Jr. Chemistry Department Endowment of the University of North Carolina as an undergraduate research participant. H. C. A. acknowledges a sabbatical leave from Clark University

## References

- (a) Permanent address: *Department of Chemistry, Clark University, Worcester, Massachusetts 01610.*  
(b) Present address: *Department of Chemistry, University of Indiana, Bloomington, Indiana 47401.*
- R. E. Dietz, F. R. Merritt, R. Dingle, D. Hone, B. G. Silbernagel and P. M. Richards, *Phys. Rev. Letters*, **26**, 1186 (1971).
- R. P. Scaringe and D. J. Hodgson, *Inorg. Chem.*, **15**, 1193 (1976).
- R. L. Lancione, H. C. Allen, Jr., and D. R. Sydor, *J. Coord. Chem.*, **4**, 153 (1975).
- R. L. Lancione and H. C. Allen, Jr., *J. Coord. Chem.*, **4**, 261 (1975).
- H. C. Allen, Jr., *J. Coord. Chem.*, **5**, 45 (1975).
- M. I. Scullane and H. C. Allen, Jr., *J. Mag. Res.*, **26**, 119 (1977).

- 8 M. I. Scullane and H. C. Allen, Jr., *J. Coord. Chem.*, **8**, 87 (1978); **8**, 93 (1978).
- 9 H. C. Allen, Jr., unpublished observations.
- 10 P. W. R. Corfield, R. J. Doedens, and J. A. Ibers, *Inorg. Chem.*, **6**, 197 (1967).
- 11 'International Tables for X-Ray Crystallography', Kynoch Press, Birmingham (1974) vol. 4.
- 12 R. F. Stewart, E. R. Davidson, and W. T. Simpson, *J. Chem. Phys.*, **42**, 3175 (1965).
- 13 D. T. Cromer and D. Liberman, *J. Chem. Phys.*, **53**, 1891 (1970).
- 14 Supplementary material is available from the Editor.
- 15 K. Iida, I. Oonishi, A. Nakahara and Y. Komiyama, *Bull. Chem. Soc., Japan*, **43**, 2347 (1970).
- 16 E. N. Baker, D. Hall and T. N. Waters, *J. Chem. Soc. A*, 400 (1970).
- 17 E. C. Lingafelter, G. L. Simmons, B. Morosin, C. Scheringer and C. Freiburg, *Acta Cryst.*, **14**, 1222 (1961).
- 18 F. J. Llewellyn and T. N. Waters, *J. Chem. Soc.*, 2639 (1960).
- 19 G. R. Clark, D. Hall and T. N. Waters, *J. Chem. Soc. A*, 223 (1968).
- 20 G. R. Clark, D. Hall and T. N. Waters, *J. Chem. Soc. A*, 823 (1969).
- 21 E. N. Baker, D. Hall and T. N. Waters, *J. Chem. Soc. A*, 396 (1970).
- 22 G. J. Palenik and J. Donohue, *Acta Cryst.*, **15**, 564 (1962).
- 23 M. Gerloch and R. Mason, *Proc. Roy. Soc., London*, **A279**, 170 (1964).
- 24 D. J. Hodgson, *Progr. Inorg. Chem.*, **19**, 173 (1975).
- 25 E. D. Estes, W. E. Hatfield, and D. J. Hodgson, *Inorg. Chem.*, **13**, 1654 (1974).
- 26 D. J. Hodgson, *Inorg. Chem.*, **15**, 3174 (1976).
- 27 P. J. Hay, J. C. Thibeault, and R. Hoffmann, *J. Am. Chem. Soc.*, **97**, 4884 (1975).
- 28 A. Bencini and D. Gatteschi, *Inorg. Chim. Acta*, **31**, 11 (1978).
- 29 B. R. McGarvey, *J. Phys. Chem.*, **71**, 51 (1967).